

# Lanthanide Complexes for Nonlinear Optics: From Fundamental Aspects to Applications

Chantal Andraud<sup>[a]</sup> and Olivier Maury<sup>\*[a]</sup>

**Keywords:** Lanthanides / Nonlinear optics / Bioimaging / Luminescence / Second harmonic generation / Two-photon absorption

Magnetic and luminescence properties of lanthanide complexes have been extensively studied; however, their potentialities in nonlinear optics (NLO) have been less explored. Since beginning of the 2000s, these properties have become an emerging field of research from the point of view of both fundamental aspects and bioimaging applications. In this microreview, we attempt to make an exhaustive compilation

of about ten years of research endeavours in lanthanide coordination chemistry and crystal engineering for nonlinear optics.

(© Wiley-VCH Verlag GmbH & Co. KGaA, 69451 Weinheim, Germany, 2009)

1. Introduction and Scope
2. Basis of NLO
3. Second-Order NLO Properties of Lanthanide Complexes
- 4 Third-Order NLO Properties of Lanthanides Complexes
5. Summary and Outlook

## 1. Introduction and Scope

Since the middle of the 20th century, lanthanides have exerted a real fascination over chemists, spectroscopists, physicists and recently biologists due to their unique chemical, magnetic and photophysical properties arising from the gradual filling of the 4f electron shell. In a first approximation, these 4f electrons are considered as core electrons with a small radial expansion shielded from the surroundings by the filled 5s<sup>2</sup>5p<sup>6</sup> shells.<sup>[1]</sup> This shielding from exter-

nal perturbations, resulting in a very small ligand- (or crystal-) field effect, is responsible for the very particular behaviour of these elements, in marked contrast with that of d-block transition metals. As a consequence, from a chemical point of view, f electrons are not (less) involved in chemical bonding, and all lanthanide(III) ions present very similar organometallic, coordination or inorganic chemistry, the small variations being due to the decreasing ionic radius upon going along a row of the periodic table (i.e. the lanthanide contraction). The metal–ligand interactions are mainly electrostatic, without any predetermined bond directionality, and complex stability is governed by an intuitive combination of steric and electronic effects, resulting in a very rich, unpredictable coordination chemistry based on polydentate and/or macrocyclic ligands.<sup>[2,3]</sup>

In addition, all Ln<sup>III</sup> ions except lanthanum and lutetium are paramagnetic, with a high-spin ground state for some of them (7/2 for gadolinium). They are therefore attractive candidates for magnetic molecular materials<sup>[4]</sup> or for particular NMR spectroscopy applications. The f electrons can present an isotropic spatial distribution, as in the case of

[a] Université de Lyon, Laboratoire de Chimie, École Normale Supérieure de Lyon, UMR 5182 CNRS, 46 allée d'Italie, 69007 Lyon, France  
E-mail: olivier.maury@ens-lyon.fr



Chantal Andraud is Research Director at the CNRS and is at the head of the “Chemistry for Optics” group in the laboratory of chemistry of École Normale Supérieure de Lyon. Her current research interests are focused on molecular engineering (organic and coordination chemistry) for different effects in optics and nonlinear optics. Targeted nonlinear effects are second harmonic generation, electro-optic effect and multiphoton absorption for electro-optic modulation, optical limiting, photodynamic therapy, biological imaging or microfabrication applications.

Olivier Maury graduated from École Nationale Supérieure de Chimie de Paris in 1993 and completed his Ph.D. in 1997 under the supervision of M. Ephritikhine (CEA Saclay). After a postdoctoral position with J.-M. Basset (CPE-Lyon), he got a CNRS position as Chargé de Recherche in 1999 at the University of Rennes in the group of H. Le Bozec. In 2004 he moved to École Normale Supérieure de Lyon to join the team of C. Andraud. His current research interests concern the design of lanthanides containing molecular materials and NIR chromophores with optimized spectroscopic properties (luminescence and nonlinear optics) towards optical limiting purposes and biological imaging applications.

the  $f^7$   $\text{Gd}^{\text{III}}$  or  $\text{Eu}^{\text{II}}$  ions, or an anisotropic one in the other cases, particularly for  $\text{Tb}^{\text{III}}$  or  $\text{Dy}^{\text{III}}$ . The anisotropic distribution induces the apparition of an anisotropic magnetic susceptibility tensor ( $\Delta\chi$ ) responsible for the permanent magnetization in single-molecule magnets<sup>[5]</sup> and for the pseudo-contact shift in NMR spectroscopy. Depending on the metal, this pseudo-contact shift can be detected as far as 40 Å away from the metal centre, which is very useful for resolving overlapping NMR signals in organic (even chiral) molecules, but also for protein structure determination.<sup>[6]</sup> On the other hand, the isotropic distribution in gadolinium results only in a broadening of the NMR spectrum due to the enhancement of electronic relaxation rates. This property has been widely exploited for the design of magnetic resonance imaging (MRI) contrast agents, which can be considered as the major breakthrough of the last 20 years in the field of medical diagnosis.<sup>[7]</sup>

The optical properties of  $\text{Ln}^{\text{III}}$  ions, which arise from 4f–4f transitions, are unique. The above-mentioned shielding of the 4f orbitals results in a very small vibrational coupling with the surroundings; consequently, f–f transitions are very narrow, characteristic of a given ion and with an emission ranging from the visible (Eu, Tb, Dy, Sm) to the near infrared (Yb, Nd, Er, but also Dy and Sm). In addition, these transitions are parity- (and sometimes spin-) forbidden, which results in very low absorption coefficients (less than  $1\text{--}3\text{ L mol}^{-1}\text{ cm}^{-1}$ ) and very long excited state lifetimes (from a few  $\mu\text{s}$  to ms). In spite of these forbidden transitions, inorganic lanthanide-doped fluorophores, such as glasses or crystals, were widely studied as laser materials (the Nd:YAG laser is one famous and well-used example) or visualization and illumination devices.<sup>[8]</sup> To overcome the drawback of the very low absorption coefficient of lanthanides, it has been demonstrated by the pioneering work of Weismann<sup>[9]</sup> that indirect population of Ln excited states is possible by excitation of a coordinated ligand followed by energy transfer to the central metal ion. This effect is called the *antenna effect*, a generic denomination that, in fact, represents many different photophysical processes: the most commonly encountered one involves as intermediate donor state the triplet excited state of a conjugated ligand or a triplet metal-to-ligand-charge-transfer state with a transition-metal-containing antenna (Figure 1).<sup>[10]</sup> Recently, sensitization by the singlet excited state of a ligand,<sup>[11]</sup> or using Ln–Ln energy transfer<sup>[12]</sup> or even sensitization by a stepwise double-electron transfer<sup>[13]</sup> have been reported. However, radiative processes are not the only possible decay modes for the lanthanide excited state, and nonradiative de-excitation pathways occur via multiphonon relaxation processes, particularly when OH or NH vibrators are coordinated to the metal ion, reducing both lifetime and quantum yield. Therefore, great synthetic efforts have been devoted to the design of antenna ligands optimizing the sensitization process for a given lanthanide ion and saturating the metal coordination sphere to avoid water or solvent coordination.<sup>[14]</sup> The luminescence of lanthanides is ubiquitous in our daily lives. They are used in particular in lamps (trichromatic lamps,<sup>[8]</sup> OLEDs<sup>[15]</sup>) or for cathodic or plasma

screens. Finally these very particular luminescence properties have been widely used in the life sciences for bioimaging<sup>[16]</sup> or biosensing<sup>[17]</sup> (tracking the presence of predetermined targets like  $\text{H}^+$ ,  $\text{Ca}^{2+}$ ,  $\text{Zn}^{2+}$ ,  $\text{HCO}_3^-$ , ...) applications. Importantly, the long excited state lifetimes of lanthanides triggered the development of time-resolved microscopy<sup>[18]</sup> or assays based on fluorescence resonance energy transfer (FRET).<sup>[19]</sup>

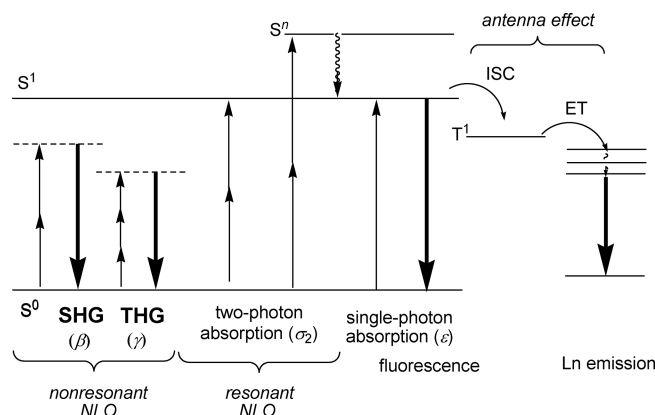


Figure 1. Jablonsky diagram representation of linear and nonlinear photophysical phenomena.

As illustrated by the large number of excellent review articles mentioned in this introduction, the study of magnetic or luminescence properties of lanthanides is a mature field of research, both from the fundamental and the application point of view. By contrast, the study of the nonlinear optics (NLO) properties of lanthanide complexes remains in its infancy, and this topic has become an emerging and also challenging field of research for the last decade. In this microreview, we attempt to propose an exhaustive description of the state-of-the-art of the design of molecular lanthanide complexes for second- or third-order NLO towards applications in biological imaging.

## 2. Basis of NLO

NLO phenomena result from the interaction between light and matter, and more precisely between the polarizable electron density (e.g. electrons of delocalized  $\pi$  systems) and the strong electric field associated with a very intense laser beam. The first experimental observations have been described in 1961 just after the development of intense laser sources, in particular by Kaiser and Garrett for two-photon absorption (vide infra)<sup>[20]</sup> and by Franken for second harmonic generation.<sup>[21]</sup>

Molecular NLO phenomena can be divided into two main classes depending on the incident laser wavelength (Figure 1): (i) *Nonresonant* NLO phenomena, such as second or third harmonic generation (SHG, THG), but also Pockel or Kerr effects, can be described as resulting from an electronic perturbation of the molecular ground state. (ii) *Resonant* NLO phenomena such as two- (or multi-) photon absorption occur only when the energy gap between the ground and excited states is a multiple of the incident

laser energy. In this case, an electron is promoted from the fundamental to the excited states by simultaneous multiphoton absorption; this is in marked contrast with nonresonant phenomena. Finally, the excited state can relax to the ground state through competing radiative and nonradiative processes, and the resulting fluorescence signal presents exactly the same characteristics as that linearly excited.<sup>[22]</sup> This two-photon-excited (induced) fluorescence phenomenon (TPEF or TPIF) is very different from up-conversion processes frequently encountered in lanthanide spectroscopy. Up-conversion processes involve either multistep excitations due to excited state absorption (ESA) or sequential energy-transfer up-conversion (ETU) evidenced by Auzel in the 1960s in Yb-Er systems.<sup>[23]</sup> This is a succession of linear excitations between real excited states from one or several moieties, whereas TPIF involves a simultaneous absorption of two photons via a virtual excited state. The frequent confusion between the two processes comes from the fact that up-conversion effects can be considered as nonlinear, due to a quadratic dependence of their efficiency on the incident intensity of the laser. Up-conversion effects will not be discussed in this review.

All these NLO phenomena (SHG, THG, TPIF) can occur simultaneously within the same material, as illustrated by the spectral response of an oriented polymer doped with DCM dye (4-dicyanomethylene-2-methyl-6-*p*-dimethylaminostyryl-4*H*-pyran) under 1.06  $\mu\text{m}$  laser irradiation (Figure 2).<sup>[24]</sup> The two sharp signals at 532 and 354 nm correspond to coherent light generated by SHG and THG, whereas the broad band is attributed to an incoherent two-photon excited fluorescence.

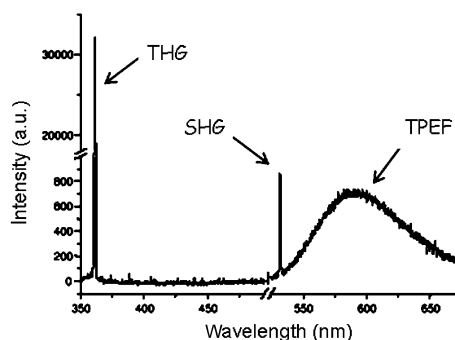


Figure 2. Spectral representation of resonant and nonresonant NLO phenomena.

Although the description of the physics behind NLO phenomena is not in the scope of this review, we will briefly detail the most relevant aspects of NLO, and the reader is invited to refer to more specialized references.<sup>[25]</sup> The interaction between the electron density of a molecule and the alternating electric field associated with a laser ( $E$ ) induces a polarization response,  $\Delta\mu$ , which can be expressed by Equation (1).

$$\Delta\mu = aE + \beta E^2 + \gamma E^3 + \dots \quad (1)$$

where  $a$ ,  $\beta$  and  $\gamma$  represent the polarizability, first-order and second-order hyperpolarizability tensors of rank 1, 2 and

3, respectively. At the macroscopic level, this equation is generalized as Equation (2).

$$\Delta P = \chi^{(1)}E + \chi^{(2)}E^2 + \chi^{(3)}E^3 + \dots \quad (2)$$

where  $\Delta P$  is the induced polarization, and  $\chi^{(1)}$ ,  $\chi^{(2)}$  and  $\chi^{(3)}$  are the first-, second- and third-order susceptibility tensors.

$\chi^{(1)}$  ( $a$  at the molecular level) belongs to the realm of linear optics; its real part is involved in the calculation of the refractive index of the medium, whereas its imaginary part determines the one-photon absorption (the extinction coefficient  $\varepsilon$  at the molecular scale).  $\chi^{(2)}$  (or  $\beta$ ) quantifies all second-order NLO effects like SHG, electro-optic effect (Pockel), frequency mixing, etc. Finally,  $\chi^{(3)}$  (or  $\gamma$ ) is representative of the third-order NLO effects such as THG, optical Kerr effect, two-photon absorption (TPA); by analogy with linear optics, its real part [ $\text{Re}(\gamma)$ ] describes the nonlinear refractive index and its imaginary part [ $\text{Im}(\gamma)$ ] the two-photon absorption cross-section ( $\sigma_2$ ).

Experimentally, the quadratic hyperpolarizability,  $\beta$ , is determined in solution by using harmonic light scattering (HLS) or electric-field-induced second harmonic generation (EFISH) techniques. For solids, Kurtz powder NLO measurements are generally performed. This semiquantitative technique is based on the comparison between the global SHG efficiency of microcrystalline samples and that of a reference (urea or KDP), but remains very sensitive to bulk sample parameters like granulometry or crystal parameters. On the other hand, two-photon cross-sections are experimentally estimated by using either the Z-scan technique or by external calibration of a TPIF excitation spectrum.<sup>[22,25]</sup>

Due to parity considerations, nonzero  $\beta$  values are restricted to noncentrosymmetric molecules and materials, while no symmetry restrictions are required for third-order NLO. Molecular engineering rules for the optimization of second-<sup>[26]</sup> or third-order<sup>[22]</sup> nonlinear optical properties have been carefully established in the case of organic molecules or conjugated polymers. As a general rule, increasing

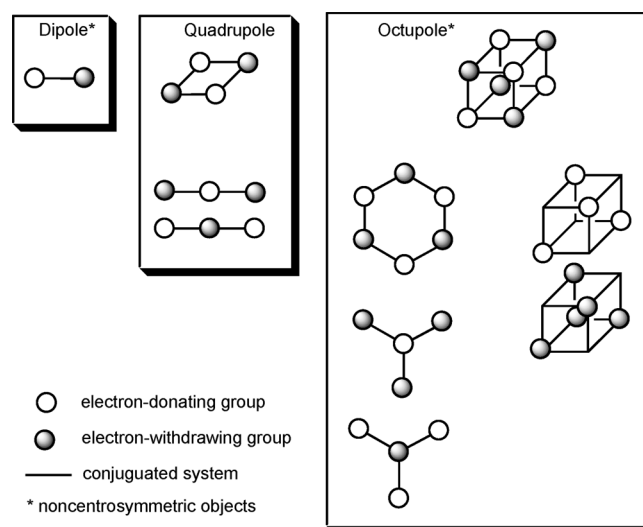


Figure 3. Schematic representation of the three main classes of NLO-phores.

the molecular electronic polarizability by the introduction of intramolecular charge transfer (CT) transitions enhances the NLO activity. It is possible to introduce one or several CT systems within a molecule, and consequently, the chromophore engineering can be divided into three main classes depending on the molecular symmetry (Figure 3): (i) the dipoles (D- $\pi$ -A), (ii) the quadrupoles (D- $\pi$ -D, A- $\pi$ -A, D- $\pi$ -A- $\pi$ -D, -A- $\pi$ -D- $\pi$ -A, ...) or (iii) the octupoles of  $D_3$  ( $A_3$ -Dcore or  $D_3$ -Acore) or  $T_d/D_{2d}$  ( $A_4$ -Dcore or  $D_4$ -Acore) symmetry (where D and A represent electron-donating and -withdrawing groups, respectively, and  $\pi$  is a conjugated skeleton). It is worth noting that only dipoles and octupoles are noncentrosymmetric and therefore suitable for second-order NLO, whereas all these systems can lead to third-order phenomena.<sup>[27]</sup> The magnitude of the CT can be modulated by the control of the strength of the donor (D) and acceptor (A), of the length and nature of the conjugated backbone ( $\pi$ ), which allows fine tuning of both linear and NLO properties.

### 3. Second-Order NLO Properties of Lanthanide Complexes

#### Inorganic Materials

Although the description of inorganic materials is beyond the scope of this review, we will report shortly SHG properties of inorganic crystalline matrices doped with rare earth ions. Noncentrosymmetric materials can be generated depending either on the symmetry of the host-crystal space group or on the distortions induced by the dopant ion. This strategy has been used for the preparation of pure inorganic materials like potassium lanthanide nitrate,  $K_2Ln(NO_3)_5$ ,<sup>[28]</sup> rare earth molybdenyl iodate  $Ln(MoO_2)(IO_3)_4(OH)$ ,<sup>[29]</sup> or mixed phosphate  $Rb_3Yb_2(PO_4)_3$ ,<sup>[30]</sup> whose NLO activity is compared to that of benchmark crystals like  $\alpha$ -quartz or KDP. For example, Townsend and co-workers used SHG to study the deformation induced by various rare earth dopants on the host bismuth germanate crystal matrix.<sup>[31]</sup> SHG measurements were conducted at the macroscopic level on waveguides doped with various lanthanide ions (Tm, Er, Ho, Eu, Sm and Nd) and normalized to a 1 wt.-% dopant ratio, assuming that the SHG signal is linearly proportional to the dopant ratio, and the results were compared to the undoped material ( $Bi_4Ge_3O_{12}$ ). For the first time, the authors underlined the influence of the nature of the lanthanide on SHG efficiency and explained their results by a size effect (Figure 4) as follows: (i) If the ionic radius of the dopant ion is close to that of the main host matrix constituent ( $Bi^{3+}$ ), which is the case for  $Eu^{3+}$ ,  $Sm^{3+}$  and to a lesser extent  $Ho^{3+}$ , the SHG signal will be similar to that of the undoped material. (ii) On the other hand, if the ionic radius of the dopant is significantly smaller ( $Tm^{3+}$  or  $Er^{3+}$ ) or larger ( $Nd^{3+}$ ), strong distortions in the crystal lattice will occur, which result in enhanced SHG signals. Finally, this substitution approach has been largely used towards the design of multifunctional materials combining laser emission

and second-order NLO properties for the preparation of self-frequency-doubling laser sources emitting at high energy with optimized concentration and crystal length.<sup>[32]</sup>

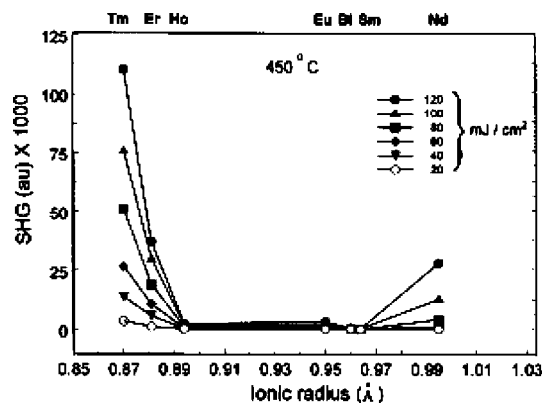


Figure 4. Evolution of the macroscopic SHG efficiency of  $Ln^{3+}$ -doped  $Bi_4Ge_3O_{12}$  crystals with the dopant ionic radius.<sup>[31]</sup>

#### Coordination Complexes

Since the first utilization of ferrocene as electron-donating group by Frazier<sup>[33]</sup> and Green,<sup>[34]</sup> metal-containing chromophores have been widely studied for second-order NLO.<sup>[35]</sup> Actually, metal-containing dipolar<sup>[36]</sup> or octupolar<sup>[37]</sup> chromophores present very strong NLO activity in the same range as that of the best organic compounds. In such systems, metal ions can play many different roles: they can act as purely donor end-groups or as purely inductive acceptor groups enforcing the intraligand charge transfer character (ILCT). In addition, they are also able to gather ligands in a predetermined geometry, giving easy access to various dipolar or octupolar symmetries.<sup>[35b]</sup> In most cases, d orbitals are involved in various low-energy optical CT transitions like metal-to-ligand (MLCT), ligand-to-metal (LMCT), metal-centred (MC), intervalence (IVCT) or more complex ligand-to-metal-to-ligand (LMLCT) charge transfer transitions. Since the global NLO activity of a complex results from the contributions of both the metal and the ligands, generally in a multidirectional way, it is very difficult to dissociate and quantify the various contributions and clearly define the role of the metal.<sup>[37a,38]</sup> It is worth noting that all studies on metal-containing chromophores have been carried out with transition metals, and almost nothing is known about the potential of lanthanide complexes in second-order NLO. This is very surprising, as the very strong chemical similarities of the lanthanide(III) ions (La–Lu) offer a unique opportunity for designing isostructural series, in which only the nature of the metal varies.

In this context, mixed organic–inorganic lanthanide-based coordination polymers offer a promising opportunity for noncentrosymmetric crystal engineering,<sup>[39]</sup> because of the high coordination number of the f elements (8, 9 and up to 12). In the early 2000s, this approach has been illustrated by Shi in the case of a polynitrile-bridged two-dimen-



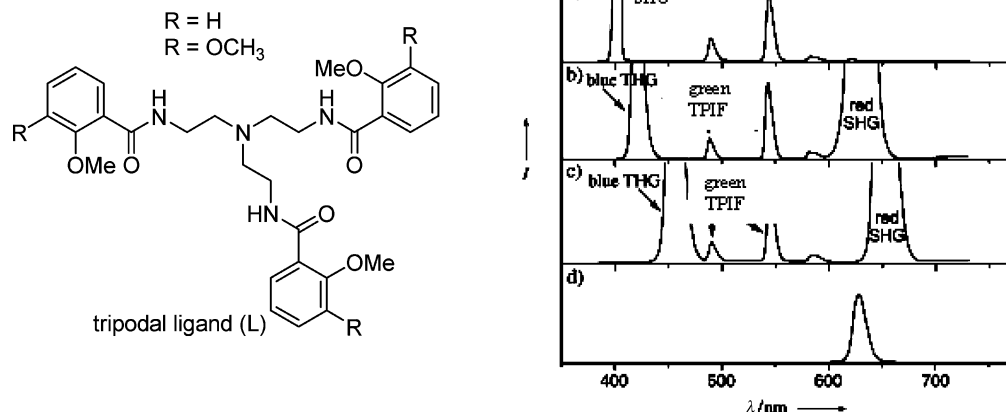


Figure 5. (left) Tripodal ligand (L); (right) emission spectra of TbL crystals under irradiation with different laser wavelengths (a)  $\lambda_{\text{ex}} = 800$  nm, (b)  $\lambda_{\text{ex}} = 1260$  nm, (c)  $\lambda_{\text{ex}} = 1340$  nm, (d) SHG spectrum of urea under 1260 nm.

sional europium polymer that crystallized in the acentric *Cc* space group, whose SHG activity was estimated to be 16.8 times that of urea (macroscopic Kurtz powder measurement).<sup>[40]</sup> More recently, Wong and collaborators reported qualitative SHG for several crystalline materials, and one representative example composed of terbium coordinated to a tripodal ligand L is depicted Figure 5.<sup>[41]</sup> In this case, SHG and THG occur simultaneously with terbium luminescence sensitized by multiphoton absorption (Figure 5 vide infra). As expected, the wavelength of the nonlinear SHG process is correlated on the incident laser irradiation wavelength (SHG occurs at 400, 630 and 670 nm for irradiation at 800, 1260 and 1340 nm, respectively), whereas the terbium luminescence wavelength remains constant, independent of the nonlinear sensitization process (namely three- or four-photon absorption). Finally, this crystal engineering approach has been successfully used for the design of multifunctional materials combining bulk NLO with magnetic properties.<sup>[42]</sup> A series of coordination polymers have been prepared of general formula  $[\text{Ln}(\text{Hfac})_3\{\text{NIT}(\text{C}_4\text{H}_6\text{OPh})\}]$  where Ln = Y, Eu, Tb, Dy, Ho, Er, Tm, Yb and NIT( $\text{C}_4\text{H}_6\text{OPh}$ ) is a nitrosyl-nitroxide radical ligand. The second-order NLO activity of the complete series, which has been estimated on microcrystalline powder, is rather low, and no influence of the rare earth elements was observed. In such systems, the macroscopic NLO contribution of the metal is negligible compared to that of the organic ligand within the supramolecular polymeric architecture.

Systematic investigations of structure–NLO-activity relationships at the molecular level of lanthanide complexes in solution are relatively scarce in the literature.<sup>[43]</sup> We described the study of two series of molecular complexes in solution: (i) a dipolar series based on a functionalized terpyridyl-like ligand, in which a charge transfer transition is induced between the dialkylaminophenyl donor group and the central pyridyl acceptor moieties<sup>[44]</sup> and (ii) an octupolar  $D_3$  symmetric series based on the dipicolinic acid (DPA) ligand (Figure 6).<sup>[45]</sup> The isostructural character of each series has been established in the solid state on the basis

of X-ray diffraction analysis, in solution by using NMR spectroscopy and thanks to theoretical calculations. As a result, each series exhibits exactly the same absorption spectra (same maximum absorption wavelength and same oscillator strength) regardless of the nature of the central metal ion. The second-order NLO measurements were performed on the dipolar and octupolar series by using the HLS technique in concentrated dichloromethane (or water) solution with nonresonant 1.91  $\mu\text{m}$  (or 1.06  $\mu\text{m}$ ) as the fundamental laser wavelength. It is worth noting that the quadratic hyperpolarizability values of the dipolar series are three orders of magnitude higher than that of the octupolar one; this huge difference can be ascribed to the absence of any charge transfer in the tris(dipicolinato)lanthanate series. But importantly, for each series, the NLO activity regularly increases from lanthanum to ytterbium or lutetium along the f-element row. Since each series is isostructural and exhibits the same absorption, this effect has been attributed to the participation of the central ion in the NLO activity and called “metal-induced NLO-enhancement”. The case of yttrium is particularly useful to get a deeper insight into this effect: yttrium belongs to group III and has no f electron as does lanthanum, but is isostructural with other lanthanides with an ionic radius between those of dysprosium and erbium. For the two series, plotting the variations of  $\beta$  with the ionic radius, as generally done for lanthanide properties, clearly reveals a discontinuity for yttrium, indicating that the NLO variations are not driven by geometrical considerations like the lanthanide contraction (Figure 6 middle). On the other hand, the very regular variation of  $\beta$  with an electronic parameter like the f electronic configuration with  $\beta(\text{Y})$  similar to  $\beta(\text{La})$  unambiguously establishes the direct contribution of f electrons to the quadratic hyperpolarizability (Figure 6, bottom). Confirmation of this effect by other groups would establish it definitively as a new general property of f-block elements.

This contribution of the f electrons to the quadratic hyperpolarizability indicates that f electrons are sensitive to an external electric field, in other words, that f electrons are polarizable, and second-order NLO techniques appear to

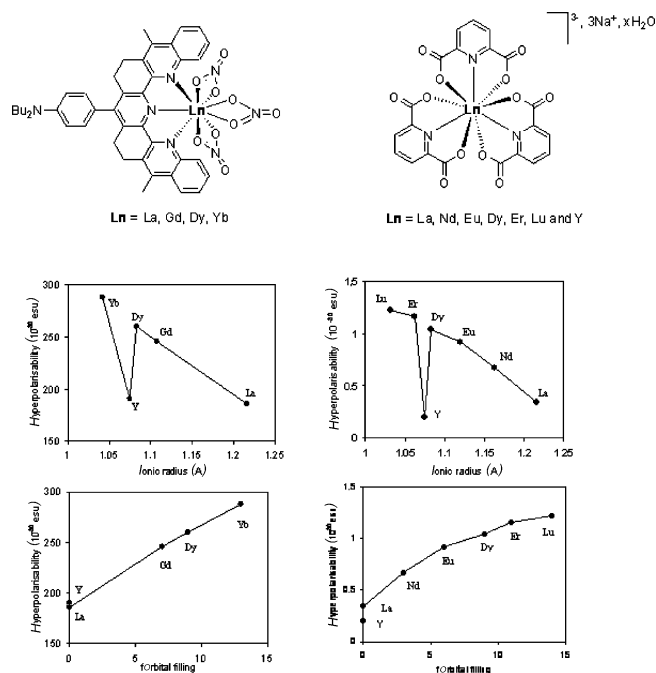


Figure 6. (top) Dipolar (left) and octupolar (right) complex structures (top), variation of the quadratic hyperpolarizability with ionic radius (middle) and f orbital filling (bottom).<sup>[44,45]</sup>

be a very sensitive tool to probe the intimate nature of the matter. This result is in marked contrast with the generally admitted (also quite dogmatic) inertness of the f electrons towards external perturbation. However, it is in good agreement with spectroscopic observations showing that this “insensitivity” of f electrons to their environment is a rough approximation since absorption, emission or NMR spectroscopic properties are strongly correlated to the local symmetry of the rare earth elements.<sup>[46]</sup> In addition, the polarizable character of f electrons was suggested in the early 1980s on the basis of X-ray diffraction and has recently been confirmed by density functional calculations.<sup>[47]</sup>

#### 4. Third-Order NLO Properties of Lanthanide Complexes

As mentioned in the introduction, third-order NLO merges under the same name very different photophysical effects, namely, (i) third harmonic generation (THG) responsible of coherent light emission at  $3\omega$  where  $\omega$  represents the incident laser wavelength, (ii) optical Kerr and nonlinear refraction effects resulting in the nonlinear modulation of the refractive index of a medium and (iii) nonlinear absorption, in which a molecule is promoted to its excited state by simultaneous absorption of two photons having half the energy corresponding to the single-photon process. This latter phenomenon is undoubtedly the most studied, because its intrinsic confocal character gives rise to a wide 3D resolved spectroscopy, photochemistry and microscopy with submicrometre precision,<sup>[22]</sup> triggering the development of numerous applications ranging from mate-

rial sciences (3D data storage, optical limiting, 3D micro-fabrication)<sup>[48]</sup> to biology (imaging, drug delivery or photodynamic therapy).<sup>[49]</sup> In this wide context, lanthanides were mainly involved in two-photon-induced luminescence applications, although some interesting papers describe marginally THG, nonlinear refraction properties or two-photon circular dichroism.

#### Third Harmonic Generation Properties

As mentioned earlier, THG has been described simultaneously with SHG and multiphoton-absorption-induced luminescence in terbium complexes of microcrystals (Figure 5).<sup>[41a]</sup> Like SHG, the wavelength of THG process varies with that of the incident laser light from 420 to 450 nm for irradiation at 1260 and 1340 nm, respectively. In addition, this coherent signal intensity exhibits the characteristic cubic dependence with the incident laser intensity.

#### Optical Kerr Effect

The third-order susceptibility of two heteroleptic triple-decker Sm mixed porphyrin-phthalocyanine molecules (Figure 7) was shown to be three orders higher than that obtained for free porphyrin and phthalocyanine, as a result of the presence of the lanthanide, which induces intermacro-cyclic interactions and TPA resonance.<sup>[50]</sup> In addition, octameric Ln (La and Ce) complexes  $[\text{Ln}_8(\text{tbzcapc})_{12}(\text{H}_2\text{O})_{24}] \cdot 6\text{dmf}$  based on the ligand tbzcapc {6-[2-N-(1,3,4-thiadiazolyl)carboxamido]-2-pyridylcarboxylate} were shown to be isostructural with discrete ellipsoid-shaped units. The third NLO properties of both complexes are completely different under fs-532 nm irradiation (Z-scan in dmf solution): the lanthanum complex presents no NLO absorption but a strong NLO refractive effect, while the cerium system exhibits NLO absorption with no NLO refractive effect. The origin of this surprising behaviour is not understood up to now.<sup>[51]</sup>

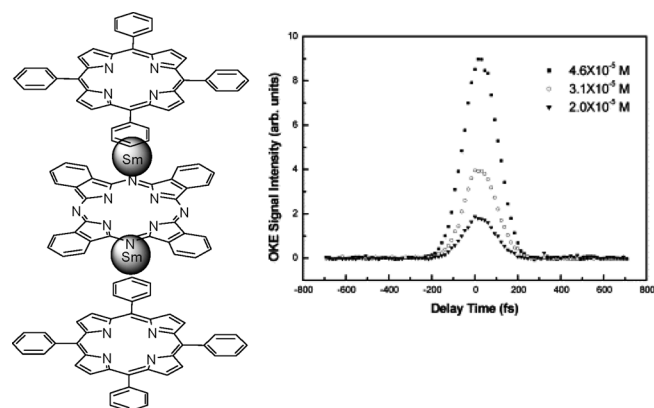


Figure 7. Triple-decker mixed porphyrin-phthalocyanine Sm complexes (left) and optical Kerr response of the porphyrin dimer at different concentrations (right).

#### Two-Photon Circular Dichroism

Richardson et al. reported studies in monoaxial crystals of  $\text{Na}_3[\text{Gd}(\text{C}_4\text{H}_4\text{O}_5)_3] \cdot 2\text{NaClO}_4 \cdot 6\text{H}_2\text{O}$  of two-photon circu-

lar dichroism (CD), which allowed to evaluate the ratio  $(\delta_L - \delta_R)/(\delta_L + \delta_R)$ , where  $\delta_L$  and  $\delta_R$  are the TPA coefficients for the crystalline material under left and right circularly polarized light, respectively; the value of this ratio is similar to those of its analogue  $(\epsilon_L - \epsilon_R)/(\epsilon_L + \epsilon_R)$  in linear CD.<sup>[52]</sup> This study, which provides information on molecular transition polarizabilities and structural data, was then rationalized and generalized in a theoretical analysis of chiral dependent TPA properties of molecules and crystals.<sup>[53]</sup>

## Two-Photon Antenna Effect in Lanthanide Complexes

Following pioneering works of Webb and co-workers,<sup>[54]</sup> two-photon laser scanning microscopy (TPLSM) is becoming a very useful tool for bioimaging purposes, particularly for thick tissue or living animals, routinely used in academic or hospital imaging platforms thanks to the availability of femtosecond-pulsed tunable lasers. The major advantage of TPLSM comes from the spectral range of excitation: indeed, the excitation is induced by simultaneous absorption of two photons having half the energy of the corresponding one-photon absorption process, and the incident wavelengths are therefore located in the infrared (700–1200 nm). In this spectral range, called “biological window”, the light is neither absorbed nor scattered by the biological tissues, allowing a deeper probing of the media (more than 500  $\mu\text{m}$ ) and limiting photo-damage of the tissue and photo-bleaching of the probe.<sup>[49,55]</sup> In this context, the design of a new generation of bioprobes combining the advantages of two-photon excitation with the unique luminescence properties of lanthanide ions (sharp emission in the visible or NIR spectral range, long excited state lifetime), is a very exciting research project involving (i) the proof-of-concept of the sensitization of lanthanide luminescence by the two-photon antenna effect, (ii) the optimization of the two-photon cross-section and (iii) the design of real bioprobes taking into account the constraints of biological media such as stability and solubility in water.

The story of TPA of lanthanides started by the first observation of two-photon-absorption-induced fluorescence phenomena in 1961 by Kaiser and Garrett in a calcium fluoride crystal doped with europium(II) ions.<sup>[20]</sup> Under a ruby laser irradiation at 694.3 nm, the blue fluorescence of  $\text{Eu}^{2+}$  at 425 nm is observed with an intensity proportional to the square of the incident laser intensity, which is a clear signature of a two-photon process (Figure 8).

Surprisingly, whereas great attention was devoted to the design and optimization of organic fluorophores, the potentialities of lanthanide complexes were forgotten for TPA applications for forty years. In the beginning of the 2000s, in a series of three papers, Lakowicz and co-workers set the main basis of this field: (i)  $\text{Eu}^{\text{III}}$  or  $\text{Tb}^{\text{III}}$  luminescence can be induced by direct two-photon excitation of the f–f transitions. (It is worth noting that f–f transitions are one-photon forbidden but two-photon allowed).<sup>[56]</sup> (ii) This multiphoton-absorption-induced lanthanide luminescence is greatly enhanced when it is sensitized by an organic ligand such as

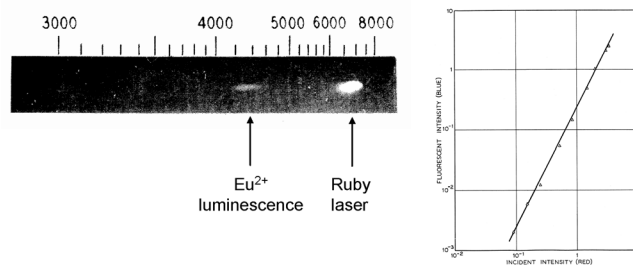


Figure 8. The first report on TPA luminescence: positive photographic plate indicating the blue emission from  $\text{CaF}_2:\text{Eu}^{2+}$  crystal under ruby laser irradiation (left) and quadric dependence of the emission intensity on the incident laser intensity (right).<sup>[20]</sup>

the tryptophan or tyrosine residue of a protein, dipicolinic acid or the coumarin-DTPA ligand (Figure 9). This is the proof-of-concept of the *two-(multi-)photon antenna effect*.<sup>[57]</sup> This antenna effect consists of an energy transfer between the organic moiety and the excited states of the lanthanide. (iii) The sensitization of lanthanide by TPA can be successfully extended to NIR emitters like ytterbium(III) bound to the aminofluorescein-DTPA ligand (Figure 9).<sup>[58]</sup>

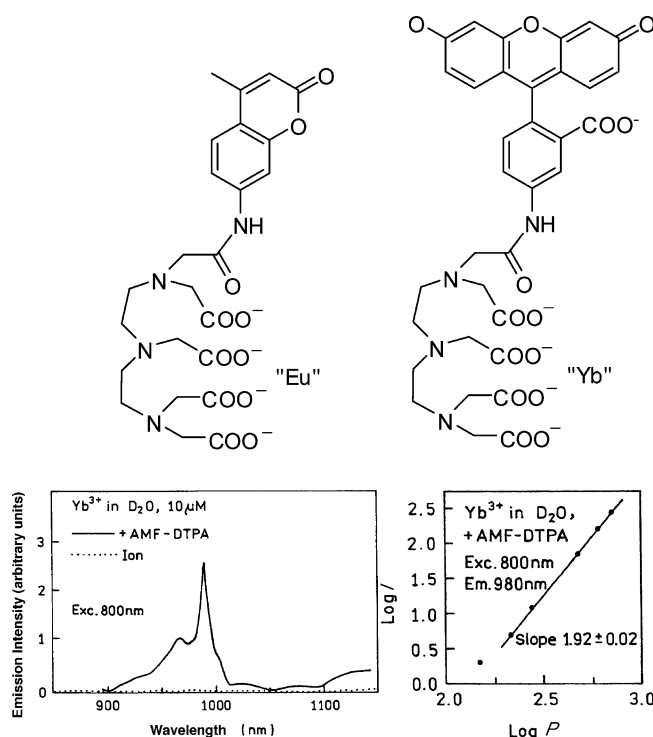


Figure 9. Structure of coumarin-DTPA and aminofluorescein-DTPA (AMF-DTPA) ligands (top). TPA-induced Yb luminescence spectra and quadratic dependence of the luminescence intensity on the incident laser power (bottom).<sup>[57,58]</sup>

From this starting point, numerous studies reported qualitatively the two-, three-, and even four-photon-absorption-sensitized luminescence of terbium bound to a protein<sup>[59]</sup> and of terbium,<sup>[41,60]</sup> europium or neodymium<sup>[61]</sup> complexes in crystal samples. The emission spectra and the excited state lifetime<sup>[41b]</sup> are rigorously the same when measured from linear or multiphoton excitation, clearly indicat-

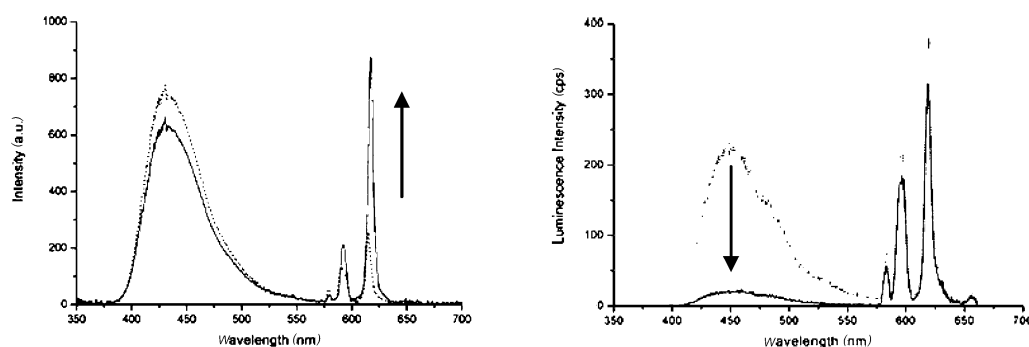
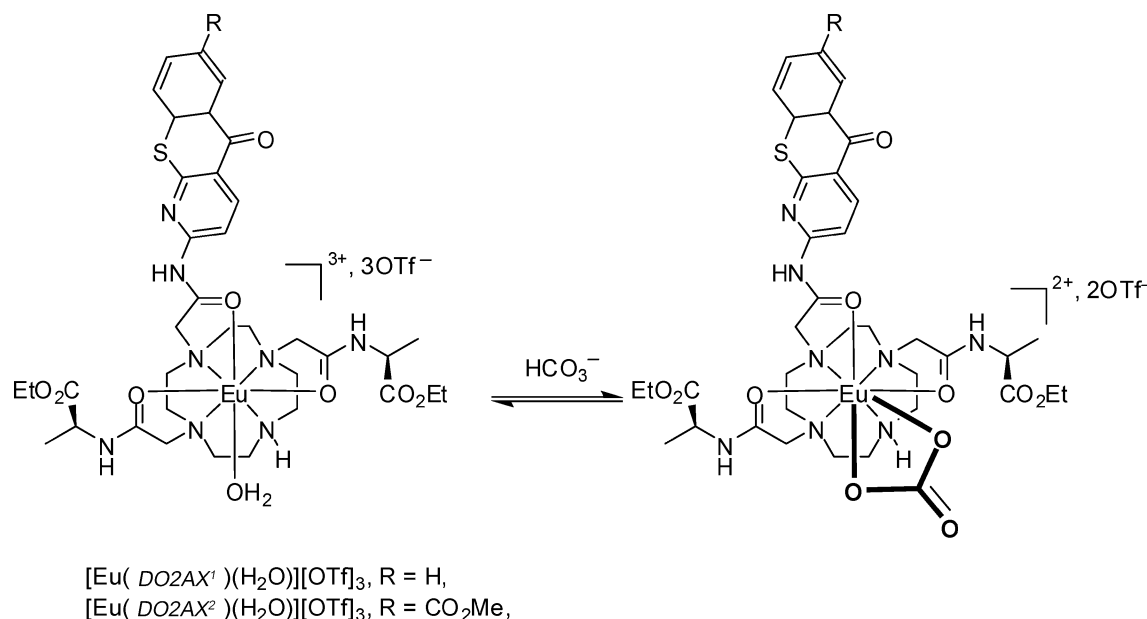


Figure 10. Top: Change in metal ion coordination upon binding  $\text{HCO}_3^-$ . Bottom: Variation of the emission spectra without (....) and with (—)  $\text{HCO}_3^-$  (right) and time-gated emission (....) of  $[\text{Eu}(\text{DO2AX})(\text{H}_2\text{O})][\text{OTf}]_3$ . The time gate had a duration of 480 ns and was delayed 75 ns with respect to the laser pulse (left).<sup>[62]</sup>

ing that the same emissive state is sensitized by both processes. In addition, Palsson and co-workers<sup>[62]</sup> reported that the sensitivity of europium(III) luminescence to its chemical environment (here  $\text{HCO}_3^-$  coordination, Figure 10), largely described for in vivo or in cellulo titration with a linear excitation,<sup>[17a]</sup> is conserved by a two-photon excitation. Moreover, in the same paper, the authors generalized the time-gated luminescence spectroscopy experiment with two-photon excitation by using a cavity-dumped Ti-sapphire source. Introducing a delay (a few hundred ns or  $\mu\text{s}$ ) between the two-photon excitation and the detection allows the elimination of any short-lived emission (Figure 10), resulting in an enhancement of the metal-centred signal-to-noise ratio. Conceptually, these two experiments are very important, because they emphasize that it is possible to conserve all the spectroscopic advantages of lanthanides while using a biphotonic excitation. However, all the aforementioned results have been obtained by using complexes, with rather low (less than 10 GM) TPA cross-sections, which represents a major drawback for practical applica-

tions. From this observation, the main challenge in this lanthanides saga concerns the optimization of the two-photon cross-section,  $\sigma_2$ .

### Optimization of the TPA Cross-Section

Molecular engineering rules for the optimization of the TPA cross-section have been carefully established in the case of organic molecules or conjugated polymers.<sup>[22,63]</sup> On the basis of these established rules, new push-pull ligands have been designed and successfully used to sensitize  $\text{Eu}^{\text{III}}$  luminescence by the two-photon antenna effect. On one hand, Werts<sup>[64]</sup> and Wang<sup>[65]</sup> independently reported dipolar tris(acetylacetonato)europium complexes bound to Michler's ketone (Mk) and functionalized bis(3,5-dimethylpyrazolyl)triazine ligands (dbpt, dmbpt), respectively; on the other hand, our group described an octupolar tris-functionalized pyridine dicarboxamide (DPAM<sup>2</sup>) complex (Figure 11).<sup>[66]</sup> All these complexes are luminescent and present



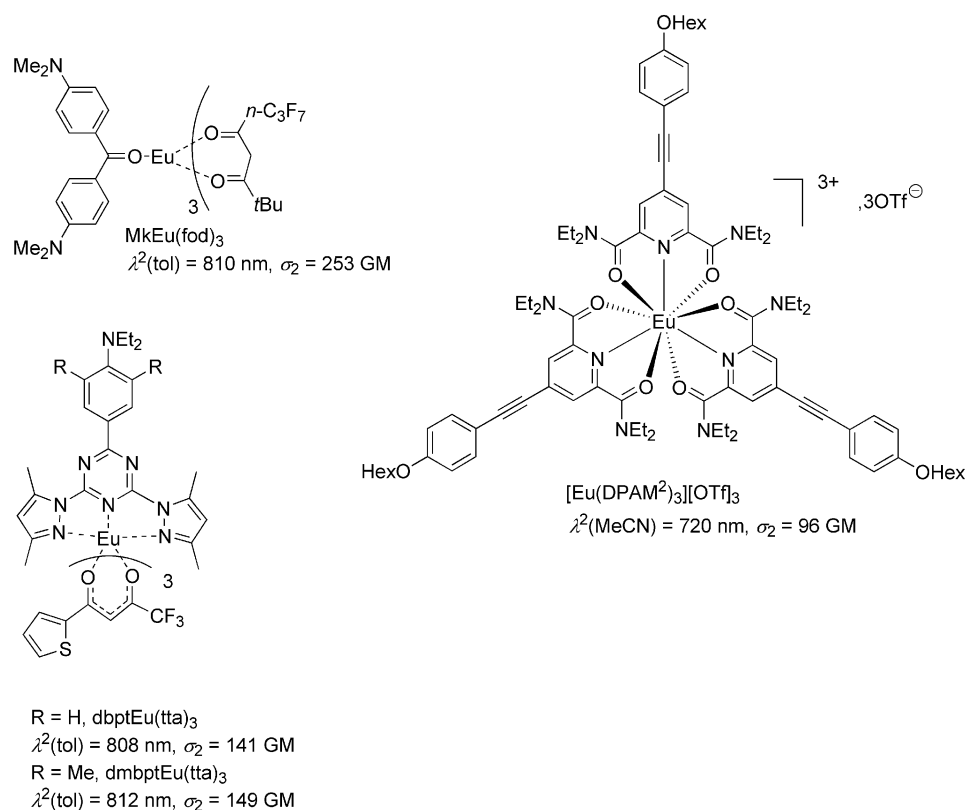
Figure 11. Structures of Eu<sup>III</sup> complexes presenting significant TPA cross-sections in organic solvents.

Table 1. Photophysical data of some lanthanide complexes for TPA applications.

Compound	Solvent	$\lambda_{\text{abs}}$ (nm)	$\Phi$	$\lambda^2$ (nm)	$\sigma_2$ (GM)	ref.
Tb <sub>2</sub> -tfr <sup>−</sup>	water			500	7.4	[59]
[Tb(DPA <sup>1</sup> ) <sub>3</sub> ] <sup>3−</sup>	water	314	0.31	< 705	26	[64]
MkEu(fod) <sub>3</sub>	tol <sup>[a]</sup>	413	0.17	810	253	[64]
dbptEu(tta) <sub>3</sub>	tol	406	0.58	808	141	[65]
dmbptEu(tta) <sub>3</sub>	tol	409	0.59	812	149	[65]
[Eu(DPAM <sup>2</sup> ) <sub>3</sub> ][OTf] <sub>3</sub>	MeCN	360	0.056	720	96	[66]
[NBu <sub>4</sub> ] <sub>3</sub> [Eu(DPA <sup>2</sup> ) <sub>3</sub> ]	DCM	321	0.15	700	14	[71]
[NBu <sub>4</sub> ] <sub>3</sub> [Eu(DPA <sup>3</sup> ) <sub>3</sub> ]	DCM	322	0.43	700	53	[71]
[NBu <sub>4</sub> ] <sub>3</sub> [Eu(DPA <sup>4</sup> ) <sub>3</sub> ]	DCM	318	0.27	740	96	[71]
[NBu <sub>4</sub> ] <sub>3</sub> [Eu(DPA <sup>5</sup> ) <sub>3</sub> ]	DCM	370	0.070	740	775	[71]
[NBu <sub>4</sub> ] <sub>3</sub> [Eu(DPA <sup>6</sup> ) <sub>3</sub> ]	DCM	427	— <sup>[b]</sup>			[71]
[NBu <sub>4</sub> ] <sub>3</sub> [Eu(DPA <sup>7</sup> ) <sub>3</sub> ]	DCM	364	0.28	730	193	[71]
[NBu <sub>4</sub> ] <sub>3</sub> [Eu(DPA <sup>8</sup> ) <sub>3</sub> ]	DCM	335	0.090	700	110	[71]
[NBu <sub>4</sub> ] <sub>3</sub> [Eu(DPA <sup>9</sup> ) <sub>3</sub> ]	DCM	335	0.036	700	218	[71]
[Na] <sub>3</sub> [Eu(DPA <sup>2G</sup> ) <sub>3</sub> ]	water	332	0.15	700	92	[75]
TbL'(NO <sub>3</sub> ) <sub>3</sub>	MeOH		0.11		3.1	[76]
[Eu(DO2AX <sup>1</sup> )(H <sub>2</sub> O)][OTf] <sub>3</sub>	water	384	0.04	770	1.7	[62]
[Eu(DO2AX <sup>2</sup> )(H <sub>2</sub> O)][OTf] <sub>3</sub>	water	372	0.008	760	0.4	[62]

[a] Abbreviation: tol = toluene, DCM = dichloromethane. [b] No Eu emission is observed.

broad intense absorption bands in the visible (above 350 nm) responsible for the two-photon absorption located in the Ti-sapphire spectral range (700–1100 nm), and, as expected, their two-photon cross-sections are significant, being in the range 100–250 GM (Table 1).

It is important to note that the presence of the CT transition induces a complete modification of the sensitization process. Generally, sensitization of lanthanide luminescence proceeds in three steps (i) singlet–singlet absorption of the

antenna ligand, (ii) intersystem crossing (ISC) to the triplet excited state (T<sub>1</sub>) and (iii) energy transfer (ET) to the metal accepting state. If the antenna ligand presents a low-energy CT transition, the sensitization can occur directly from the relaxed CT state without any participation of the triplet. This possibility, suggested in the cases of MkEu(fod)<sub>3</sub><sup>[67]</sup> and [Eu(DPAM<sup>2</sup>)<sub>3</sub>][OTf]<sub>3</sub>,<sup>[66]</sup> has been nicely demonstrated for dpbtEu(tta)<sub>3</sub> (Figure 12).<sup>[11b]</sup> Time-resolved luminescence experiments show that the decay time constant of the

CT-state emission (1.8 ns) matches exactly with the rise time constant of the  $^5D_1$  state, whereas the triplet  $T_1$  state exhibits at 77 K a phosphorescence lifetime of 3.9 s, which is far higher than that of europium emission (0.65 ms) (Figure 12). The same sensitization process, also established for other Eu complexes<sup>[11,68]</sup> and generalized to NIR emitters<sup>[11c,69]</sup> (Yb, Nd), can now be considered as a new general property of CT transitions.

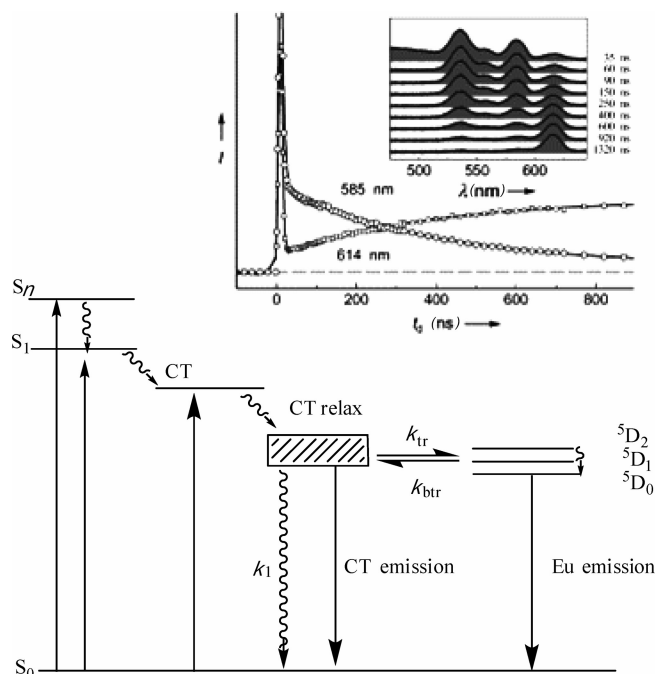


Figure 12. Schematic representation of the direct CT-sensitization process where  $k_{tr}$  and  $k_{btr}$  are the rate constants of energy transfer and back transfer, respectively.<sup>[11c]</sup> Inset: decay-to-rise time correlation for dbptEu(tta)<sub>3</sub>.<sup>[11b]</sup>

In spite of their significant TPA cross-section, all the above-mentioned complexes (Figure 11) are only stable in organic solvents, and therefore no practical application as fluoroprobe for bioimaging microscopy can be envisaged. In this context, the TPA cross-section optimization on a functionalized tris(dipicolinato)lanthanide series presenting good water solubility was undertaken.<sup>[70]</sup> A complete series of dipolar ligands D- $\pi$ -A (DPA<sup>2-9</sup>) and the corresponding [NBu<sub>4</sub>]<sub>3</sub>[Eu(DPA<sup>i</sup>)<sub>3</sub>] ( $i = 2-9$ ) complexes were studied, in which the acceptor part (A) is the dipicolinic acid fragment and the strength of the donor (D = dialkylamino, alkoxy, alkylthio) as well as the length of the  $\pi$ -conjugated backbone [phenyl, phenylethynyl, naphthylethynyl, bis(phenylethynyl), chalcone] have been tuned (Figure 13).<sup>[11c,71]</sup> In this case also, the direct sensitization of Eu<sup>III</sup> through the CT excited state of the ligand was confirmed. In addition, the global efficiency of this sensitization process (in term of quantum yield or lifetime) varies dramatically with the energy of this CT excited state.<sup>[11c]</sup> Maximum efficiency is obtained for [NBu<sub>4</sub>]<sub>3</sub>[EuDPA<sup>3</sup>], featuring a weak donor alkylthio moiety, when the CT transition is close to the europium  $^5D_1$  accepting state. On the contrary, a very strong decrease is observed when the CT transition approaches the

emissive  $^5D_0$  excited state (e.g. in [NBu<sub>4</sub>]<sub>3</sub>[EuDPA<sup>5</sup>]<sub>3</sub>) featuring a stronger dialkylamino donor group). Further decrease of the CT energy ([NBu<sub>4</sub>]<sub>3</sub>[EuDPA<sup>6</sup>]<sub>3</sub>) definitely hinders the sensitization process. On the other hand, the TPA cross-section increases monotonically with the decrease in the CT-state energy of the ligand (Table 1). In other words, as observed for organic molecules, increasing the donor strength or lengthening the conjugated backbone significantly enhances the TPA cross-section and redshifts the maximum TPA wavelength. For [NBu<sub>4</sub>]<sub>3</sub>[EuDPA<sup>5</sup>]<sub>3</sub>, a record value of 775 GM at 740 nm has been obtained. This can be considered close to the upper limit that can be reached for this family of complexes. Indeed, although higher  $\sigma_2$  values should be expected by further extension of the  $\pi$  system, for example, the resulting lower gap between the antenna and the Eu excited state will prohibit any energy transfer to the metal, as in [NBu<sub>4</sub>]<sub>3</sub>[Eu(DPA<sup>6</sup>)<sub>3</sub>]. It is important to note that this upper limit depends of course on the nature of the lanthanide ion and higher  $\sigma_2$  values can be envisaged for NIR emitting lanthanides, whereas lower limit values are expected for Tb or Dy, for which accepting excited states lie at higher energy.

For practical use of lanthanide complexes as bioprobes, the problem is not to consider complexes that present only a giant TPA cross-section, but to find systems with the best compromise between TPA activity and luminescence quantum yield,  $\phi$ ; for this purpose, the challenge consists of the optimization the *two-photon brightness*,  $B^{(2)} = \sigma_2 \times \phi$ . An alternative approach is to confine spatially the luminescent molecules within nano-objects like dendrimers, polymers or particles. This strategy has been successfully used for organic molecules and giant two-photon cross-sections up to several thousand of GM, resulting from the addition of the molecular contributions, have been reached.<sup>[72]</sup> In this context, Wang recently reported the synthesis of silica nanoparticles doped with dbptEu(tta)<sub>3</sub> with a homogeneous size distribution (ca. 40 nm in diameter).<sup>[73]</sup> Due to the concentration effect, the doped nanoparticle two-photon cross-section was estimated to be 320 000 GM at 832 nm [for an average loading of about  $8.5 \times 10^3$  dbptEu(tta)<sub>3</sub> complex molecules per particle]. Such a type of nano-object fulfils the requirement in terms of stability, good dispersibility and high nonlinear efficiency in water and should be extremely promising for two-photon scanning microscopy experiments.

## Towards Bioimaging Applications

The proof-of-concept two-photon microscopy experiment with lanthanide complexes has been established by using a tris(dipicolinato)terbium complex in crystals or in protein-derived crystals.<sup>[74]</sup> In spite of the very low TPA efficiency of this complex, the microscopy experiment was successful as a result of the high concentration of luminescent species in the crystal and under confocal irradiation at 532 nm, only a small glowing point was observed in the middle of one crystal plate (Figure 14). Inspired by the

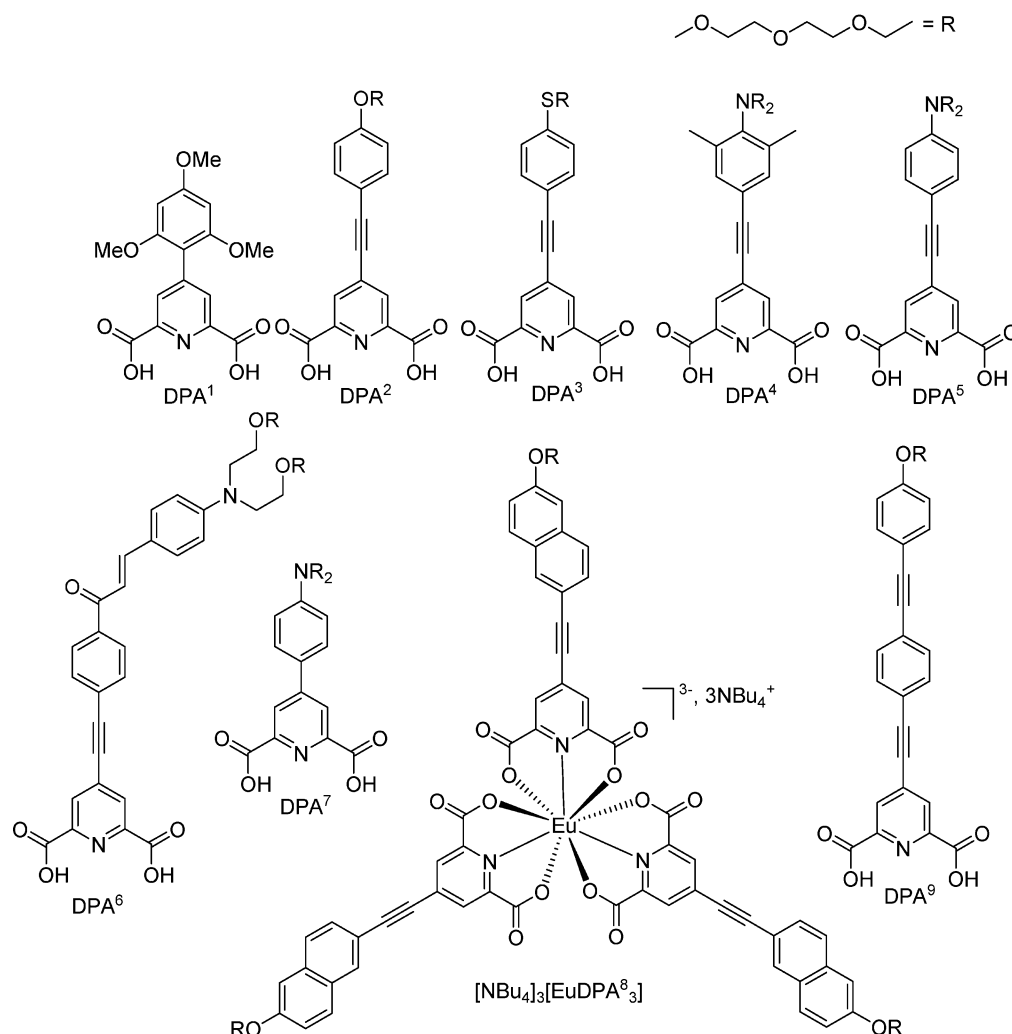


Figure 13. Structure of functionalized dipicolinato ligands and related lanthanide complexes.

above-mentioned optimization study, we designed a new complex,  $[\text{Na}]_3[\text{EuDPA}^{2\text{G}}_3]$ , in which the ligand is functionalized by an alkoxyphenylethynyl system, and the hydro-solubility is ensured by 3,4,5-tris(triethyleneglycol)phenyl moieties and by the sodium counteranions.<sup>[75]</sup> This complex is soluble and stable enough in water and exhibits a good quantum yield (0.157) and a significant TPA cross-section (92 GM at 700 nm). By using this complex as bioprobe, two-photon scanning microscopy experiments were carried out on fixed cancer cells with 760 nm laser irradiation (Figure 15). The images exhibit a nice signal-to-noise ratio, and nucleus, nucleoli and endoplasmic reticulum are clearly visible. It is worth noting that, in this case, both excitation and detection are located in the red, a spectral range where the biological medium is more transparent, which is a major advantage for in-depth investigation. At the same time, Wong and co-workers described in vitro cell imaging by using three-photon excitation of  $\text{TbL}'(\text{NO}_3)_3$  {where  $\text{L}'$  designates a tripodal ligand,  $N$ -[2-(bis{2-[(3-methoxybenzoyl)amino]ethyl}amino)ethyl]-3-methoxybenzamide}.<sup>[76]</sup> In spite of rather low two- (or three-) photon activity (Table 1), this complex does not present any cytoto-

xicity for various kinds of cells, which makes it possible to image living cells (Figure 16). A few months later, Parker and co-workers reported the first practical utilization of two-photon scanning microscopy with a terbium complex featuring an azaxanthone antenna chromophore as a probe.<sup>[77]</sup> The purpose of these studies was to determine the cellular localization profile and emission quenching sensitivity as a function of probe substitution (ester, acid, amide, alkyl organic fragment or LysArg<sub>7</sub>, Arg<sub>7</sub>, guanidinium or human serum albumin conjugated link). In these papers, the two-photon microscopy with lanthanide complexes is becoming the tool that can be used to carry out bioimaging research projects. The very short delay between the proof-of-concept experiments and the first practical utilization clearly underlines the high potentiality of this new generation of fluoroprobe for bioimaging applications. However, many improvements remain to be achieved: (i) the optimization of the two-photon cross-section in biological media in the 780–820 nm wavelength range, (ii) the design of two-photon bioprobes based on NIR emitters (Yb, Nd, etc.) and (iii) the development of biphotonic time-resolved bioimaging techniques.

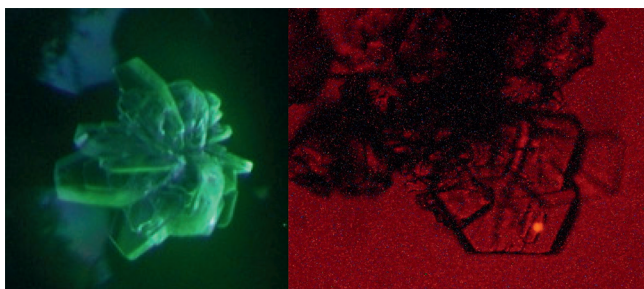


Figure 14. Linear microscopy imaging (UV irradiation at 365 nm) of a lysozyme-derivative-crystal containing tris(dipicolinato)terbium (left), nonlinear two-photon microscopy under 532 nm laser irradiation (right).

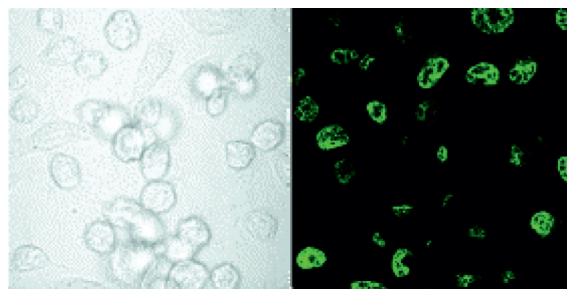


Figure 16. Three-photon confocal fluorescence microscopy imaging of human nasopharyngeal carcinoma live cells incubated with terbium complexes.

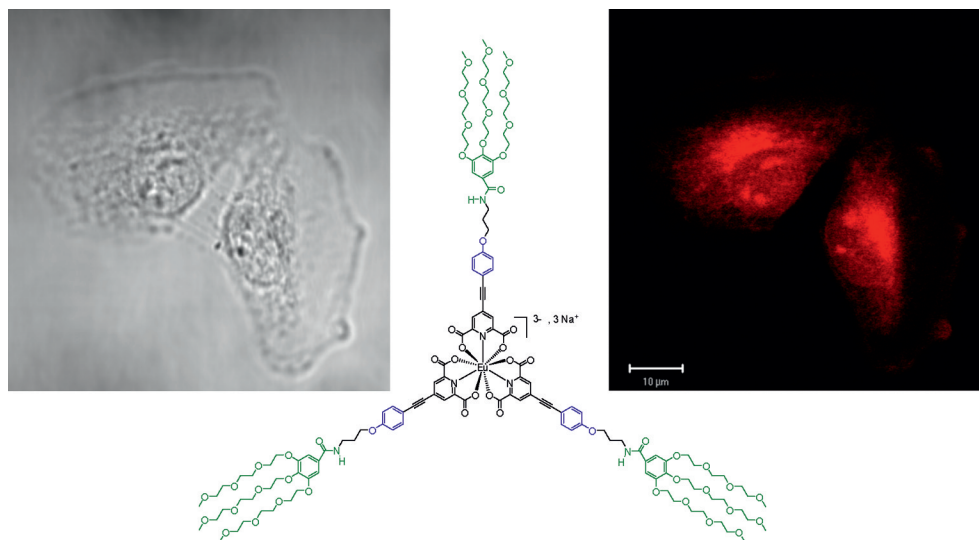


Figure 15. Structure of the  $[\text{Na}]_3[\text{EuDPA}^{2\text{G}}_3]$  bioprobe (middle). Images of fixed cancer cells obtained by using the techniques of phase contrast (left) and two-photon excitation (right).

## 5. Summary and Outlook

At the end of this literature survey covering the last ten years, it appears that the investigation of lanthanide NLO properties is a growing and exciting field of research. During this first decade, fundamental properties have been found and different proofs-of-concept have been established. The second-order NLO properties of organic materials were generally limited to the polarizable nature of delocalized systems based on  $\pi$  electrons, and the discovery of the direct contribution of  $f$  electrons to the quadratic hyperpolarizability led to expand the scope of this field of research. A complete rationalization of this phenomenon and its physical modelling remain to be established. From a chemical point of view, the (hyper)polarizable character of  $f$  electrons, in agreement with many other spectroscopic observations, call into question the inertness of these electrons towards their environment, and NLO appears as a powerful tool to probe the intimate nature of the matter. On the other hand, it has been clearly demonstrated that lanthanide luminescence can be sensitized efficiently by two-photon absorption<sup>[78]</sup> with efficiencies comparable to those of organic compounds. In addition, the proofs-of-concept of

TPA time-gated spectroscopy and lanthanide-based TPA scanning microscopy have been established. Much research is still necessary to combine high TPA cross-sections with improved stability in biological media, low cytotoxicity and efficient cellular uptake or target imaging. However, all these results open the way for the design of new optimized bioprobes and nonlinear microscopy set-ups suitable to combine the advantage of TPA excitation with the unique lanthanide luminescence properties. In particular, lanthanide bioprobes will present promising perspectives for bioimaging of thick tissues with original time-resolved nonlinear microscopy techniques.

## Acknowledgments

This project started in Rennes and became possible thanks to the trust of Hubert Le Bozec who contributed significantly in the second-order NLO study. The experimental work from our group has been performed with the help of very talented graduate students and postdocs: Katell Sénéchal, Christophe Feuvrie, Adrien Bourdolle, Alexandre Picot, Anthony D'Aléo and Mustapha Allali. We are very grateful for their outstanding contribution. EFISH and



HLS experiments were performed in collaboration with Prof. J. Zyss and Prof. I. Ledoux-Rak (ENS Cachan), TPA measurements with Dr. P. L. Baldeck (University of Grenoble), NIR lifetime measurement with Dr. A. Beeby and J. A. G. Williams (University of Durham), and bioimaging experiments are carried out in collaboration with Dr. A. Grishine and A. Duperray (INSERM, Grenoble); we are greatly indebted to all of them. Finally we are grateful to Centre National de la Recherche Scientifique (CNRS), ENS-Lyon, Région Rhône-Alpes and French ANR programme (ANR LnOnL NT05-3\_42676) for financial support.

- [1] A. J. Freeman, R. E. Watson, *Phys. Rev.* **1962**, *127*, 2058.
- [2] For selected reviews see, a) T. Gunlaugsson, F. Stomeo, *Org. Biomol. Chem.* **2007**, *5*, 1999–2009; b) H. C. Aspinall, *Chem. Rev.* **2002**, *102*, 1807–1850; c) J.-C. G. Bünzli, C. Piguet, *Chem. Rev.* **2002**, *102*, 1897–1928; d) D. Parker, R. S. Dickins, H. Pushmann, C. Crossland, J. A. K. Howard, *Chem. Rev.* **2002**, *102*, 1977–2010; e) V. Alexander, *Chem. Rev.* **1995**, *95*, 273–342.
- [3] a) N. Kaltsoyannis, P. Scott, *The f Elements*, Oxford Univ. Press, Oxford, **1999**; b) S. Cotton, *Comprehensive Coordination Chemistry II*, Elsevier, Amsterdam, **1994**, vol. 3, pp. 93–188.
- [4] C. Benelli, D. Gatteschi, *Chem. Rev.* **2002**, *102*, 2369–2387.
- [5] For recent examples see: a) M. A. Al Daman, J. M. Clemente-Juan, E. Coronado, C. Martí-Gastaldo, A. Gaita-Arino, *J. Am. Chem. Soc.* **2008**, *130*, 8874–8875; b) C. Aronica, G. Pillet, G. Chastanet, W. Wernsdorfer, J.-F. Jacquot, D. Luneau, *Angew. Chem. Int. Ed.* **2006**, *45*, 4659–4662.
- [6] a) G. Pintacuda, M. John, X.-C. Su, G. Otting, *Acc. Chem. Res.* **2007**, *40*, 206–212; b) M. Allerozzi, I. Bertini, M. B. L. Janik, Y.-M. Lee, G. Liu, C. Luchinat, *J. Am. Chem. Soc.* **2000**, *122*, 4154–4161.
- [7] a) P. Caravan, J. J. Ellison, T. J. McMurphy, R. B. Lauffer, *Chem. Rev.* **1999**, *99*, 2293–2352; b) P. Hermann, J. Kotek, V. Kubicek, I. Lukes, *Dalton Trans.* **2008**, 3027–3047.
- [8] T. Jüstel, H. Nikol, C. Ronda, *Angew. Chem. Int. Ed.* **1998**, *37*, 3084–3103.
- [9] S. I. Weissman, *J. Chem. Phys.* **1942**, *10*, 214–217.
- [10] M. D. Ward, *Coord. Chem. Rev.* **2007**, *251*, 1663–1677.
- [11] a) G. A. Hebbink, S. I. Klink, L. Grave, P. G. Oude Alink, F. C. J. M. van Veggel, *ChemPhysChem* **2002**, *3*, 1014–1018; b) C. Yang, L.-M. Fu, Y. Wang, J.-P. Zhang, W.-T. Wong, X.-C. Ai, Y.-F. Qiao, B.-S. Zou, L.-L. Gui, *Angew. Chem. Int. Ed.* **2004**, *43*, 5010–5013; c) A. D'Aléo, A. Picot, A. Beeby, J. A. G. Williams, B. Le Guennic, C. Andraud, O. Maury, *Inorg. Chem.* **2008**, *47*, 10258–10268.
- [12] S. Faulkner, S. J. A. Pope, *J. Am. Chem. Soc.* **2003**, *125*, 10526–10527.
- [13] a) W. D. W. Horrocks, J. P. Bolender, W. D. Smith, R. M. Supkowski, *J. Am. Chem. Soc.* **1997**, *119*, 5972–5973; b) A. Beeby, S. Faulkner, J. A. G. Williams, *J. Chem. Soc., Dalton Trans.* **2002**, 1918–1922.
- [14] For general reviews see: a) A. De Bettencourt-Dias, *Curr. Org. Chem.* **2007**, *11*, 1460–1480; b) M. H. V. Werts, *Science Prog.* **2005**, *88*, 101–131; c) J.-C. G. Bünzli, C. Piguet, *Chem. Soc. Rev.* **2005**, *34*, 1048–1077; d) D. Parker, *Chem. Soc. Rev.* **2004**, *33*, 156–165.
- [15] a) A. de Bettencourt-Dias, *Dalton Trans.* **2007**, 2229–2241; b) J. Kido, Y. Okamoto, *Chem. Rev.* **2002**, *102*, 2357–2368.
- [16] S. Faulkner, S. J. A. Pope, B. P. Burton-Pye, *Appl. Spectrosc. Rev.* **2004**, *39*, 1–35.
- [17] a) S. Pandya, J. Yu, D. Parker, *Dalton Trans.* **2006**, 2757–2766; b) T. Gunlaugsson, J. P. Leonard, *Chem. Commun.* **2005**, 3114–3131; c) D. Parker, *Coord. Chem. Rev.* **2000**, *205*, 109–130.
- [18] a) J. Yuan, G. Wang, *J. Fluoresc.* **2005**, *15*, 559–568; b) A. Beeby, S. W. Botchway, I. M. Clarkson, S. Faulkner, A. W. Parker, D. Parker, J. A. G. Williams, *J. Photochem. Photobiol. B: Biology* **2000**, *57*, 83–89; c) G. Marriot, R. M. Clegg, D. J. Arnt-Jovin, T. Jovin, *Biophys. J.* **1991**, *60*, 1374–1387.
- [19] a) I. Hemmilä, S. Webb, *Drug Discovery Today* **1997**, *2*, 373–381; b) L. J. Charbonière, N. Hildebrandt, *Eur. J. Inorg. Chem.* **2008**, 3241–3251.
- [20] W. Kaiser, C. G. B. Garrett, *Phys. Rev. Lett.* **1961**, *7*, 229–231.
- [21] P. A. Franken, A. E. Hill, C. W. Peters, *Phys. Rev. Lett.* **1961**, *7*, 118–119.
- [22] G. S. He, L.-S. Tan, Q. Zheng, P. N. Prasad, *Chem. Rev.* **2008**, *108*, 1245–1330.
- [23] F. Auzel, *Chem. Rev.* **2004**, *104*, 139–173.
- [24] Courtesy of S. Brasselet, unpublished results.
- [25] a) D. S. Chemla, J. Zyss (Eds.), *Nonlinear Optical Properties of Organic Molecules and Crystals*, Academic Press, Orlando, **1987**; b) N. P. Prasad, D. J. Williams, *Introduction to Nonlinear Optical Effects in Molecules and Polymers*, Wiley, New York, **1991**; c) J. Zyss, *Molecular Nonlinear Optics: Materials, Physics and Devices*, Academic Press, Boston, **1994**; d) H. S. Nalwa, S. Miyata (Eds.), *Nonlinear Optics of Organic Molecules and Polymers*, CRC Press, Boca Raton, **1997**.
- [26] D. M. Burland, *Chem. Rev.* (special issue) **1994**, *94*, 1–278.
- [27] J. Zyss, I. Ledoux, *Chem. Rev.* **1994**, *94*, 77–105.
- [28] W. Dong, H. Zhang, Q. Su, Y. Lin, S. Wang, C. Zhu, *J. Solid State Chem.* **1999**, *148*, 302–307.
- [29] T. C. Shehee, R. E. Sykora, K. M. Ok, P. S. Halasyamani, T. E. Albrecht-Schmitt, *Inorg. Chem.* **2003**, *42*, 457–462.
- [30] J. J. Carvajal, I. Pareu, R. Solé, X. Solans, F. Díaz, M. Aguiló, *Chem. Mater.* **2005**, *17*, 6746–6754.
- [31] a) A. K. Jazmati, G. Vasquez, P. D. Townsend, *Nucl. Inst. Meth. Phys. Res. B* **2000**, *166–167*, 592–596; b) P. D. Townsend, A. K. Jazmati, T. Karali, M. Maghrabi, S. G. Raymond, B. Yang, *J. Phys. Condens. Matter* **2001**, *13*, 2211–2224.
- [32] For a review, see: A. Brenier, *J. Lumin.* **2000**, *91*, 121–132.
- [33] C. C. Frasier, M. A. Harvey, M. P. Cokerham, H. M. Hand, E. A. Chauchard, C. H. Lee, *J. Phys. Chem.* **1986**, *90*, 5703–5706.
- [34] M. L. H. Green, S. R. Marder, M. E. Thompson, J. A. Bandy, D. Bloor, P. V. Kolinsky, R. J. Jones, *Nature* **1987**, *330*, 360–362.
- [35] a) N. J. Long, *Angew. Chem. Int. Ed. Engl.* **1995**, *34*, 21–38; b) I. R. Whittall, A. M. McDonagh, M. G. Humphrey, M. Samoc, *Adv. Organomet. Chem.* **1998**, *42*, 291–362; I. R. Whittall, A. M. McDonagh, M. G. Humphrey, M. Samoc, *Adv. Organomet. Chem.* **1999**, *43*, 349–405; c) P. G. Lacroix, *Eur. J. Inorg. Chem.* **2001**, 339–348; d) T. Renouard, H. Le Bozec, *Eur. J. Inorg. Chem.* **2001**, 229–239; e) S. Di Bella, *Chem. Soc. Rev.* **2001**, *30*, 355–366; f) B. J. Coe, *Comprehensive Coordination Chemistry II* (Eds.: J. A. McCleverty, T. J. Meyer), Elsevier Pergamon, Oxford, **2004**, vol. 9, pp. 621–687; g) C. E. Powell, M. G. Humphrey, *Coord. Chem. Rev.* **2004**, *248*, 725–756; h) O. Maury, H. Le Bozec, *Acc. Chem. Res.* **2005**, *38*, 691–704.
- [36] a) S. M. Le Cours, H.-W. Guan, S. G. DiMaggio, C. H. Wang, M. J. Therien, *J. Am. Chem. Soc.* **1996**, *118*, 1497–1503; b) T.-G. Zhang, Y. Zhao, I. Asselberg, A. Persoons, K. Clays, M. J. Therien, *J. Am. Chem. Soc.* **2005**, *127*, 9710–9720; c) V. Alain, M. Blanchard-Desce, C.-T. Chen, S. R. Marder, A. Fort, M. Barzoukas, *Synth. Met.* **1996**, *81*, 133–136; d) Y. Liao, B. E. Eichinger, K. A. Firestone, M. Haller, J. Luo, W. Kaminsky, J. B. Benedict, P. J. Reid, A. K.-Y. Jen, L. R. Dalton, B. H. Robinson, *J. Am. Chem. Soc.* **2005**, *127*, 2758–2766.
- [37] a) O. Maury, L. Viau, K. Sénéchal, B. Corre, J.-P. Guégan, T. Renouard, I. Ledoux, J. Zyss, H. Le Bozec, *Chem. Eur. J.* **2004**, *10*, 4454–4466; b) L. Viau, S. Bidault, O. Maury, S. Brasselet, I. Ledoux, J. Zyss, E. Ishow, K. Nakatani, H. Le Bozec, *J. Am. Chem. Soc.* **2004**, *126*, 8386–8387; c) S. Bidault, L. Viau, O. Maury, S. Brasselet, J. Zyss, E. Ishow, K. Nakatani, H. Le Bozec, *Adv. Funct. Mater.* **2006**, *16*, 2252–2262.
- [38] a) D. R. Kanis, P. G. Lacroix, M. A. Ratner, T. J. Marks, *J. Am. Chem. Soc.* **1994**, *116*, 10089–10102; b) S. D. Cummings, L.-T. Cheng, R. Eisenberg, *Chem. Mater.* **1997**, *9*, 440–450; c) F. W. Vance, J. T. Hupp, *J. Am. Chem. Soc.* **1999**, *121*, 4047–4053; d) J. B. Gaudry, L. Capes, P. Langot, S. Marcen, M.

- Kollmansberger, O. Lavastre, E. Freysz, J.-F. Letard, O. Kahn, *Chem. Phys. Lett.* **2000**, 324, 321–329; e) B. J. Coe, J. A. Harris, B. S. Brunschwig, I. Asselberghs, K. Clays, J. Garin, J. Orduna, *J. Am. Chem. Soc.* **2005**, 127, 13399–13410; f) F. Tessoro, D. Roberto, R. Ugo, M. Pizzotti, S. Quici, M. Cavazzini, S. Bruni, F. De Angelis, *Inorg. Chem.* **2005**, 44, 8967–8978.
- [39] Many articles deal with crystal engineering with organic or transition-metal-containing compounds: see, for example, a) V. R. Thalladi, S. Brasselet, H.-C. Weiss, D. Bläser, A. K. Katz, H. L. Carrell, R. Boese, J. Zyss, A. Nangia, G. R. Desiraju, *J. Am. Chem. Soc.* **1998**, 120, 2563–2577; b) O. R. Evans, W. Lin, *Acc. Chem. Res.* **2002**, 35, 511–522.
- [40] J.-M. Shi, W. Xu, Q.-Y. Liu, F.-L. Liu, Z.-L. Huang, H. Lei, W.-T. Yu, Q. Fang, *Chem. Commun.* **2002**, 756–757.
- [41] a) K.-L. Wong, G.-L. Law, W.-M. Kwok, W.-T. Wong, D. L. Phillips, *Angew. Chem. Int. Ed.* **2005**, 44, 3436–3439; b) G.-L. Law, W.-M. Kwok, W.-T. Wong, K.-L. Wong, P. A. Tanner, *J. Phys. Chem. B* **2007**, 111, 10858–10861.
- [42] L. Bogani, L. Cavigli, K. Bernot, R. Sessoli, M. Gurioli, D. Gatteschi, *J. Mater. Chem.* **2006**, 16, 2587–2592.
- [43] NLO-inactive lanthanate anions have been used as bulky spacers in stilbazonium-containing Langmuir–Blodgett films, but no effect of the metal was reported: a) K. Z. Wang, C. H. Huang, G. X. Xu, Y. Xu, Y. Q. Liu, D. B. Zhu, X. S. Zhao, X. M. Xie, N. Z. Wu, *Chem. Mater.* **1994**, 6, 1986–1989; b) C. H. Huang, K. Wang, G. Xu, X. Zhao, X. Xie, Y. Xu, Y. Liu, L. Xu, T. Li, *J. Phys. Chem.* **1995**, 99, 14397–14402; c) K. Wostyn, K. Binnemans, K. Clays, A. Persoons, *J. Phys. Chem. B* **2001**, 105, 5169–5173.
- [44] a) K. Sénéchal, L. Toupet, I. Ledoux, J. Zyss, H. Le Bozec, O. Maury, *Chem. Commun.* **2004**, 2180–2181; b) K. Sénéchal-David, A. Hemeryck, N. Tancrez, L. Toupet, J. A. G. Williams, I. Ledoux, J. Zyss, A. Boucekkinne, J.-P. Guégan, H. Le Bozec, O. Maury, *J. Am. Chem. Soc.* **2006**, 128, 12243–12255.
- [45] N. Tancrez, C. Feuvrie, I. Ledoux, J. Zyss, L. Toupet, H. Le Bozec, O. Maury, *J. Am. Chem. Soc.* **2005**, 127, 13474–13475.
- [46] a) S. T. Frey, W. D. J. Horrock, *Inorg. Chim. Acta* **1995**, 383–390; b) D. Parker, *Chem. Soc. Rev.* **2004**, 33, 156–165 and references cited therein; c) L. Di Bari, G. Pintacuda, P. Salvadori, R. S. Dickins, D. Parker, *J. Am. Chem. Soc.* **2000**, 122, 9257–9264.
- [47] E. Furet, K. Costuas, P. Rabiller, O. Maury, *J. Am. Chem. Soc.* **2008**, 130, 2180–2183 and references cited therein.
- [48] a) C. W. Spangler, *J. Mater. Chem.* **1999**, 9, 2013–2020; b) C. Andraud, R. Fortrie, C. Barsu, O. Stéphan, H. Chermette, P. L. Baldeck, *Adv. Polym. Sci.* **2008**, 214, 149–203; c) K.-S. Lee, R. H. Kim, D.-Y. Yang, S. H. Park, *Prog. Polym. Sci.* **2008**, 33, 631–681; d) C. N. LaFratta, J. T. Fourkas, T. Baldacchini, R. A. Farrer, *Angew. Chem. Int. Ed.* **2007**, 46, 6238–6258.
- [49] a) W. R. Zipfel, R. M. Williams, W. W. Webb, *Nat. Biotechnol.* **2003**, 21, 1369–1377; H. M. Kim, B. R. Cho, *Acc. Chem. Res.* **2009**, 42, 863–872.
- [50] W. Huang, H. Xiang, Q. Gong, Y. Huang, C. Huang, J. Jiang, *Chem. Phys. Lett.* **2003**, 374, 639–644.
- [51] H. Hou, Y. Wei, Y. Song, Y. Fan, Y. Zhu, *Inorg. Chem.* **2004**, 43, 1323–1327.
- [52] K. E. Gunde, F. S. Richardson, *Chem. Phys.* **1995**, 194, 195–206.
- [53] K. E. Gunde, G. W. Burdicka, F. S. Richardson, *Chem. Phys.* **1996**, 208, 195–218.
- [54] W. Denk, J. H. Strickler, W. W. Webb, *Science* **1990**, 248, 73–76.
- [55] For reviews see: a) R. Yuste, *Nat. Methods* **2005**, 2, 902–904; b) J. Mertz, *Curr. Opin. Neurobiol.* **2004**, 14, 610–616; c) P. J. Campagnola, L. M. Loew, *Nat. Biotechnol.* **2003**, 21, 1356–1360.
- [56] J. R. Lakowicz, G. Piszczek, B. P. Maliwal, I. Gryczynski, *ChemPhysChem* **2001**, 2, 247–252.
- [57] G. Piszczek, B. P. Maliwal, I. Gryczynski, J. Dattelbaum, J. R. Lakowicz, *J. Fluoresc.* **2001**, 11, 101–107.
- [58] G. Piszczek, I. Gryczynski, B. P. Maliwal, J. R. Lakowicz, *J. Fluoresc.* **2002**, 12, 15–17.
- [59] G. F. White, K. L. Litvinenko, S. R. Meech, D. L. Andrew, A. J. Thompson, *Photochem. Photobiol. Sci.* **2004**, 3, 47–55.
- [60] a) W. P.-W. Lai, W.-T. Wong, B. K.-F. Li, K.-W. Cheah, *New J. Chem.* **2002**, 26, 576–581; b) L. Luo, W. P.-W. Lai, K. L. Wong, W.-T. Wong, K.-F. Li, K.-W. Cheah, *Chem. Phys. Lett.* **2004**, 398, 372–376; c) K.-L. Wong, G.-L. Law, W. M. Kwok, W.-T. Wong, D. L. Phillips, *Angew. Chem. Int. Ed.* **2005**, 44, 3436–3439.
- [61] G.-L. Law, K.-L. Wong, Y.-Y. Yang, H.-L. Yang, W.-T. Wong, M. H.-W. Lam, H.-L. Tam, K.-W. Cheah, *J. Fluoresc.* **2008**, 18, 749–752.
- [62] L.-O. Palsson, R. Pal, B. S. Murray, D. Parker, A. Beeby, *Dalton Trans.* **2007**, 5726–5734.
- [63] a) M. Pawlicki, H. A. Collins, R. G. Denning, H. L. Anderson, *Angew. Chem. Int. Ed.* **2009**, 48, 3244–3266; b) H. M. Kim, B. R. Cho, *Chem. Commun.* **2009**, 153–193.
- [64] M. H. V. Werts, N. Nerambourg, D. Pélégry, Y. Le Grand, M. Blanchard-Desce, *Photochem. Photobiol. Sci.* **2005**, 4, 531–538.
- [65] a) L.-M. Fu, X.-F. Wen, X.-C. Ai, Y. Sun, Y.-S. Wu, J.-P. Zhang, Y. Wang, *Angew. Chem. Int. Ed.* **2005**, 44, 747–750; b) R. Hao, M. Li, Y. Wang, J. Zhang, Y. Ma, L. Fu, X. Wen, Y. Wu, X. Ai, S. Zhang, Y. Wei, *Adv. Funct. Mater.* **2007**, 17, 3663–3669.
- [66] A. Picot, F. Malvotti, B. Le Guennic, P. L. Baldeck, J. A. G. Williams, C. Andraud, O. Maury, *Inorg. Chem.* **2007**, 46, 2659–2665.
- [67] M. H. V. Werts, M. A. Duin, J. W. Hofstraat, J. W. Verhoeven, *Chem. Commun.* **1999**, 799–800.
- [68] a) Y. H. Kim, N. S. Baek, H. K. Kim, *ChemPhysChem* **2006**, 7, 213–221; b) D. Nie, Z. Chen, Z. Bian, J. Zhou, Z. Liu, F. Y. Z. Chen, C. Huang, *New J. Chem.* **2007**, 31, 1639–1646; c) P. Kad-jane, L. Charbonnière, F. Camerel, P. P. Lainé, R. Ziessel, *J. Fluoresc.* **2008**, 18, 119–129.
- [69] N. M. Shavaleev, R. Scopelliti, F. Gumy, J.-C. G. Bünzli, *Eur. J. Inorg. Chem.* **2008**, 1523–1529.
- [70] A.-L. Gassner, C. Duhot, J.-C. G. Bünzli, A.-S. Chauvin, *Inorg. Chem.* **2008**, 47, 7802–7812 and references cited therein.
- [71] A. D'Aléo, A. Picot, P. L. Baldeck, C. Andraud, O. Maury, *Inorg. Chem.* **2008**, 47, 10269–10279.
- [72] a) F. Stellacci, C. A. Bauer, T. Meyer-Friedrichsen, W. Wenseleers, S. R. Marder, J. W. Perry, *J. Am. Chem. Soc.* **2003**, 125, 328–329; b) O. Mongin, T. R. Krishna, M. H. V. Werts, A.-M. Caminade, J.-P. Majoral, M. Blanchard-Desce, *Chem. Commun.* **2006**, 915–917; c) S. Kim, H. E. Pudavar, P. N. Prasad, *Chem. Commun.* **2006**, 2071–2073; d) S. Kim, H. E. Pudavar, A. Bonoio, P. N. Prasad, *Adv. Mater.* **2007**, 19, 3791–3795; e) L. Bertazza, L. Celotti, G. Fabbrini, M. A. Loi, M. Maggini, F. Mancini, S. Marcuz, E. Menna, M. Muccini, U. Tonellato, *Tetrahedron* **2006**, 62, 10434; f) S. Kim, T. Y. Ohulchanskyy, H. E. Pudavar, R. K. Pandey, P. N. Prasad, *J. Am. Chem. Soc.* **2007**, 129, 2669–2675.
- [73] X. Wen, M. Li, Y. Wang, J. Zhang, L. Fu, R. Hao, Y. Ma, X. Ai, *Langmuir* **2008**, 24, 6932–6936.
- [74] A. D'Aléo, G. Pompidor, B. Elena, J. Vicat, P. L. Baldeck, L. Toupet, R. Kahn, C. Andraud, O. Maury, *ChemPhysChem* **2007**, 8, 2125–2132.
- [75] A. Picot, A. D'Aléo, P. L. Baldeck, A. Grishine, A. Duperray, C. Andraud, O. Maury, *J. Am. Chem. Soc.* **2008**, 130, 1532–1533.
- [76] G. L. Law, K.-L. Wong, C. W.-Y. Man, W.-T. Wong, S.-W. Tsao, M. H.-W. Lam, P. K.-S. Lam, *J. Am. Chem. Soc.* **2008**, 130, 3714–3715.
- [77] a) F. Kielar, A. Congreve, G.-L. Law, E. J. New, D. Parker, L.-L. Wong, P. Castreno, J. De Mendoza, *Chem. Commun.* **2008**, 2435–2437; b) F. Kielar, G.-L. Law, E. J. New, D. Parker, *Org. Biomol. Chem.* **2008**, 6, 2256–2258.

[78] During the preparation of this manuscript, two additional articles dealing with TPA sensitization of europium complexes were published: a) P. Kadjane, M. Starck, F. Camerel, D. Hill, N. Hildebrandt, R. Ziessel, L. J. Charbonniere, *Inorg. Chem.*

**2009**, 48, 4601–4603; b) M. Shi, C. Ding, J. Dong, H. Wang, Y. Tian, Z. Hu, *Phys. Chem. Chem. Phys.* **2009**, 11, 5119–5123.

Received: June 15, 2009

Published Online: September 22, 2009